1-1-2015

N719- and D149-sensitized 3D hierarchical rutile TiO2 solar cells - a comparative study

Jianjian Lin
University of Wollongong, jl824@uowmail.edu.au

Yoon-Uk Heo
Pohang University of Science and Technology

Andrew Nattestad
University of Wollongong, anattest@uow.edu.au

Mohammed Shahabuddin
King Saud University

Yusuke Yamauchi
National Institute For Materials Science, Waseda University

See next page for additional authors

N719- and D149-sensitized 3D hierarchical rutile TiO2 solar cells - a comparative study

Abstract

Poor dye loading on rutile TiO_2 is one of the chief reasons for lower solar-to-electric conversion efficiency (η) in dye-sensitized solar cells (DSCs), compared to their anatase based counterparts. Previously, we showed that similar light harvesting for both rutile and anatase was realized by using a metal-free organic indoline dye, D149 [Sci. Rep., 2014, 4, 5769]. This was in contrast to the bulk of previous studies, which employed ruthenium based N719, leading to significant differences in light harvesting. To date, there has been no report directly comparing N719 and D149 for rutile based DSCs. In this work, three-dimensional hierarchical rutile TiO_2 architecture (HRTA), consisting of one-dimensional nanorods, was successfully prepared via a facile hydrothermal method, and subsequently optimized as effective photoelectrodes for DSCs. Two dyes, N719 and D149, were used as sensitizers of the HRTA-based DSCs, with maximum η of 5.6% and 5.8% achieved, respectively. The higher η of the D149-sensitized DSC is ascribed to its higher extinction co-efficient, allowing a greater amount of light to be harvested with a thinner TiO_2 layer. This study suggests that some of the limitations typically observed for rutile TiO_2 based DSCs can be overcome through the use of strongly absorbing metal-free organic sensitizers. Furthermore, it reemphasises the importance of viewing DSCs as whole systems, rather than individual components.

Keywords

sensitized, study, 3d, comparative, hierarchical, rutile, tio2, solar, cells, n719, d149

Disciplines

Engineering | Physical Sciences and Mathematics

Publication Details

Lin, J., Heo, Y., Nattestad, A., Shahabuddin, M., Yamauchi, Y. & Kim, J. Ho. (2015). N719- and D149-sensitized 3D hierarchical rutile TiO_2 solar cells - a comparative study. Physical Chemistry Chemical Physics, 17 (11), 7208-7213. Physical Chemistry Chemical Physics

Authors

Jianjian Lin, Yoon-Uk Heo, Andrew Nattestad, Mohammed Shahabuddin, Yusuke Yamauchi, and Jung Ho Kim

A Comparative Study of N719- and D149-sensitized 3D Hierarchical Rutile TiO_2 Solar Cells

Jianjian Lin,[a] Yoon-Uk Heo,[b] Andrew Nattestad,[c,*] Yusuke Yamauchi,[d] Shi Xue Dou,[a] and Jung Ho Kim[a,*]

[a]*Institute for Superconducting and Electronic Materials (ISEM), Australian Institute for Innovative Materials (AIIM), University of Wollongong, North Wollongong, NSW 2500, Australia*
Tel: +61-2-4298-1420. E-mail: jhk@uow.edu.au
[b]*Graduate Institute of Ferrous Technology, Pohang University of Science and Technology, San 31, Hyoja-Dong, Pohang 790-784, Republic of Korea*
[c]*Intelligent Polymer Research Institute (IPRI), ARC Centre of Excellence for Electromaterials Science, AIIM, University of Wollongong, North Wollongong, NSW 2500, Australia*
Tel: +61-2-4298-1456. E-mail: anattest@uow.edu.au
[d]*World Premier International (WPI) Research Center for Materials Nanoarchitectonics (MANA), National Institute for Materials Science (NIMS), 1-1 Namiki, Tsukuba , Ibaraki 305-0044, Japan*

ABSTRACT

Poor dye loading on rutile TiO_2 is one of the chief reasons for lower solar-to-electric conversion efficiency (η) in dye-sensitized solar cells (DSCs), compared to their anatase based counterparts. Previously, we showed that similar light harvesting for both rutile and anatase was realized by using a metal-free indoline dye, D149. This was in contrast to the bulk of previous studies, which employed ruthenium based N719, leading to significant differences in light harvesting. To date, there has been no report directly comparing N719 and an organic dye (D149) for rutile based DSCs. In this work, a three-dimentional hierarchical rutile TiO_2 architecture (HRTA), consisting of one-dimensional nanorods, was successfully prepared via a facile hydrothermal method, and subsequently optimized as effective photoelectrodes for DSCs. Two dyes, N719 and D149, were used as sensitizers of the HRTA-based DSCs, with maximum η of 5.6 % and 5.8 % achieved, respectively. The higher η of D149-sensitized DSC is ascribed to its higher extinction co-efficient, allowing a greater amount of light to be harvested with a thinner TiO_2 layer. This study suggests that some of the limitations typically observed for rutile TiO_2 based DSCs can be overcome through the use of strongly absorbing metal-free organic sensitizers. Further, it reemphasises the importance of viewing DSCs as whole systems, rather than individual components.

1. Introduction

Renewable energy resources continue to gain attention due to increasing global energy demands, limited access to fossil fuels, and an increasing awareness of the negative impacts of these carbon based resources. In the field of renewable energy, dye-sensitized solar cells (DSCs) have attracted significant attention, with much research conducted to enhance the efficiency of DSCs by developing or modifying individual DSC components, such as sensitizers, photoanodes, electrolytes, and counter electrodes. As one of the key elements of the DSC, substantial research efforts have been focused on building TiO_2 micro/nanostructures with high surface area to provide improved charge transport while facilitating good light harvesting. Different TiO_2 architectures in the forms of 1D (tubes, wires, fibres, rods), 2D (sheets, belts), and 3D (spheres, trees, flowers) nanostructures have been developed, and to date, large size TiO_2 structures have been extensively used as scatterers to improve the light harvesting efficiency of DSCs.

Less attention has been paid to rutile, especially three-dimensional (3D) hierarchical rutile architectures for use in DSCs. It is the authors' opinion that rutile has been ignored due to perceived issues such as its more positive conduction band edge potential, which are expected to result in lower open-circuit voltages (V_{oc}) than for anatase. Previous studies[ref] have, however, shown that rutile-based DSCs can attain a similar V_{oc} to those made with anatase. In this case, device performance seems to be mainly hindered by lower dye loading. In our previous study,[ref] we demonstrated that similar light harvesting for both rutile and anatase coule be realized by using a metal-free indoline dye, D149, with a high peak extinction co-efficient (68700 M^{-1} cm^{-1} at 526 nm), hence comparable efficiencies were obtained. As yet there are no reports (to the best of our knowledge) comparing N719 and D149 rutile based DSCs. It is hoped that this work will demonstrate that the observed shortfalls of rutile are not inherent. Furthermore, it is hoped

that this research will help to illustrate the importance of viewing a DSC as a system, rather than a collection of individual parts.

In this work, we report a modified 3D hierarchical rutile TiO_2 architecture (HRTA), which consists of one-dimensional (1D) nanorods that were self-assembled to form microspheres, which were successfully prepared via a facile hydrothermal method without any surfactant or template, and optimized as an effective photoelectrode for DSCs. Two commercially available dyes, a ruthenium complex, N719 and a metal-free organic indoline D149, were used as sensitizers, with maximum solar-to-electric conversion efficiency (η) of 5.6 % and 5.8 % achieved, respectively. The higher η of D149-sensitized DSC is ascribed to its higher molar extinction co-efficient. Hence, metal-free organic D149 sensitizer can be considered as a better candidate for low-cost rutile-based DSC application.

2. Experimental

2.1 Synthesis of 3D Hierarchical Rutile TiO_2 Architectures (HRTA)

Tetrabutyl titanate ($Ti(OCH_2CH_2CH_2CH_3)_4$, 97 %, TT, analytical reagent grade) and hydrochloric acid (37 % HCl, analytical reagent grade) were purchased from Sigma-Aldrich, and used without purification or additives. HRTA was prepared via a modified acid thermal process[ref]. Briefly, 1.0 mL of TT, was added dropwise into 25 mL HCl (1M) at room temperature whilst under stirring (with stirring maintained for 1.5 h). This solution was then transferred to a Teflon lined reactor (Parr Instrument Company, 45 mL) and sealed, then heated to 150 $^{\circ}$C for 5 h. Afterwards, the sample was cooled before being centrifuged and washed with ethanol three times, and finally the samples were dried at 90 $^{\circ}$C overnight under vacuum.

2.2 Preparation of Photoanodes

Photoanodes were prepared in a manner similar to that reported previously.[ref] Briefly, A dense TiO_2 layer [using spray pyrolysis of a titanium (IV) diisoproxide-*bis*-acetylacetonate

(75 wt % in isopropanol, Aldrich) solution (dilution 1:9 in ethanol) at 450 °C] was firstly applied on top of F: SnO_2 (FTO) glass. Then a layer of TiO_2 paste was cast onto the FTO glass plates by the doctor-blade method. Then the electrodes were subjected to a sintering process (150 °C for 10 min, 325 °C for 5 min, 375 °C for 5 min, 450 °C for 30 min, 500 °C for 15 min). Finally the TiO_2 films were soaked in 0.02 M aqueous titanium tetrachloride solution ($TiCl_4$) at 70 °C for 30 min.

2.3 Fabrication of DSCs

The porous TiO_2 films were immersed in a 0.5 mM D149 (1-material, Canada) dye solution [1:1 (v/v) mixture of acetonitrile (HPLC, Lab-scan) and *tert*-butanol (LR, Ajax Chemicals)] or in a 0.5 mM N719 (Solaronix) dye solution [1:1 (v/v) mixture of *tert*-butanol (LR, Ajax Chemicals) and acetonitrile (HPLC, Lab-scan)] for overnight once their temperature decreased to approximately 110 °C. The photoelectrode was sandwiched together with the counter electrode [coated with one drop of 10 mM platinic acid solution (H_2PtCl_6 , Sigma)], using a 25 µm Surlyn (Solaronix) spacer. The I^-/I_3^- organic solvent based electrolyte solution [50 mM iodine (Sigma), 0.6 M 1,2-dimethyl-3-propylimidazelium iodide (Solaronix), 0.1 M lithium iodide (Sigma) in methoxypropionitrile (Sigma) for D149] [acetonitrile/valeronitrile (85:15 vol %), iodine (I_2) (0.03 M), 4 tertbutylpyridine (4-tBP) (0.5 M), 1-butyl-3-methylimidazolium iodide (BMII) (0.6 M), and guanidinium thiocyanate (GuSCN) (0.1 M) for N719] was introduced into the filling port by a vacuum back-filling technique.

2.4 Characterization

XRD was employed to examine the crystal structures of the resultant products using an X-ray diffractometer (Bruker Advance, 40 kV, 30 mA) (Cu Kα, λ = 0.15406 nm) from 5º to 80º (2θ) (1 º/min), while the morphology was examined by FE-SEM (Megallan 200) and TEM (JEM-2100F). The surface area and porosity were examined using Brunauner-Emmet-Teller (BET) analysis of nitrogen adsorption-desorption data collected on a Tristar 3030 system

(Micrometrics Instrument Corporation), after degassing overnight at 150 °C. A Veeco Dektak 150 Surface Profiler was used for the film thickness measurements. A Keithley 2400 sourcemeter was used for photocurrent density - voltage (*J-V*) curve measurements, under air mass (AM) 1.5 global (1.5G) one sun illumination (100 mW cm^{-2}). A 300 W Xe lamp was used for incident photon-to-current quantum conversion efficiency (IPCE) measurements, a monocromator with sorting filters focused on a spot with additional optics. A Keithley 2400 SMU was used for recording the short circuit current response of the devices (5 nm steps). The measured currents were referenced to a calibrated Si photodiode (PECCELL). Electrochemical impedance spectroscopy (EIS) was performed at open circuit under illumination (0.1-1.0 MHz).

3. Results and Discussions

Fig. 1(a, b) shows scanning electron microscope (SEM) and dark-field transmission electron microscope (DF-TEM) images of the 3D hierarchical rutile TiO_2 architecture (HRTA), synthesized by a facile hydrothermal treatment of a solution of 1.0 mL titanium butoxide (TB) and 25 mL hydrochloric acid (HCl), at 150 °C for 5 h.[ref] Compared to our previous work, the increased quantity of titanium butoxide (from 0.5 mL to 1.0 mL) can be seen to result in more textured hierarchical spheres with diameters of ~ 200 nm, which are much smaller than previous ones (~ 1-1.5 µm). Furthermore, the average specific surface area is higher than in our previous report (84 compared to 67 m^2g^{-1}), [ref] which is further discussed below. It can be seen from high magnification SEM images of a full particle [Fig. 1(c)] and a fractured one [Fig. 1(d)] that the structure is constructed from many radially structured, dendritic, and densely packed crystalline nanorods.

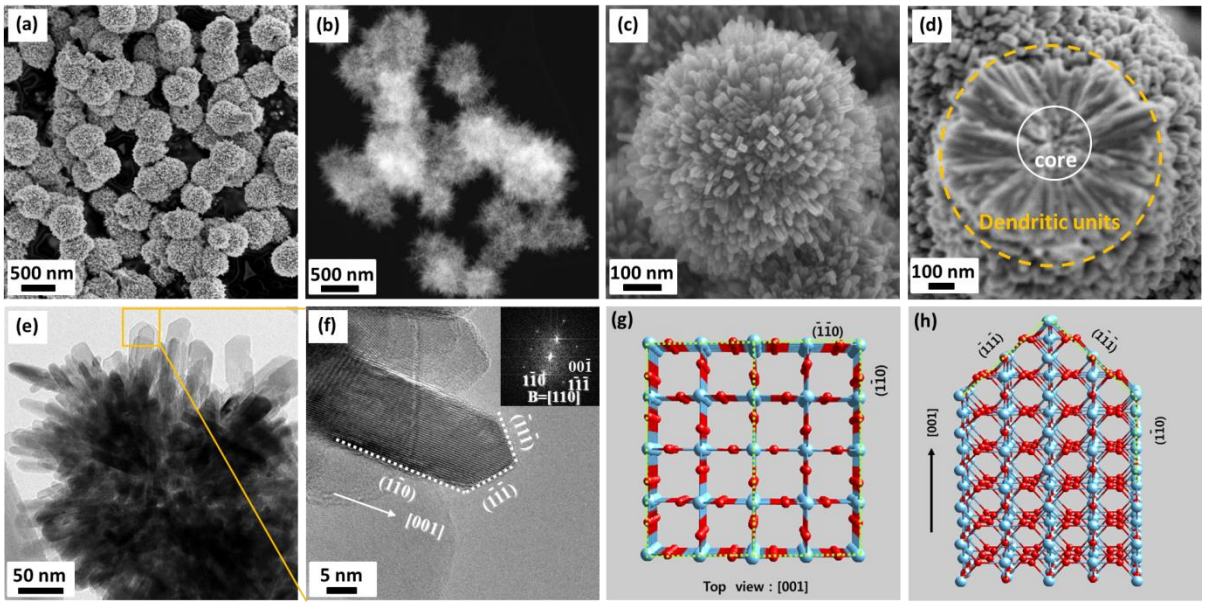

Figure 1. (a) Low magnification SEM image and (b) DF STEM image of 3D hierarchical rutile TiO_2 architecture (HRTA). (c) SEM image of an individual HRTA microsphere. (d) SEM image of a fractured microsphere. (e) TEM image of a quarter microsphere. (f) TEM image of individual nanorod; inset: corresponding SAED pattern. (g, h) atomic structure of a rutile nanorod.

Fig. 1(e, f) shows TEM images of a small fraction of one microsphere and a typical nanorod, respectively. The nanorod appears to be a 1D tetragonal prism with a width of 10 nm, similar to the SEM observations. The nanorods have a high aspect ratio (~ 20), calculated from an average width of ~ 10 nm and a diameter of ~ 200 nm. The structure of the corresponding selected area electron diffraction (SAED) pattern is shown in the inset of Fig. 1(f), confirming the nanorods to be single-crystal rutile TiO_2 structures, in agreement with the X-ray diffraction (XRD) pattern [Fig. S1(a) in the Supporting Information (SI)], the Raman spectrum [Fig. S1(b)], and high-resolution TEM (HRTEM) image[Fig. S1(c)].

SAED also reveals that the cuboid crystal facets are parallel to [110], and the pyramid-shaped crystal facets are parallel to [111], indicating that preferred growth takes place along the [001] direction, with the atomic structure as shown in Fig. 1(g, h). In general, the (110) crystal plane is perpendicular to the (001) crystal plane, and thus the nanorods grow along the (110) crystal plane with a preferred [001] orientation. It is reasonable to assume that the TiO_2

nanorod preferentially exposes the {110} side facets and the {111} top facets and grows along the [001] direction on the basis of above results together with the XRD pattern.

Brunauer-Emmett-Teller (BET) analysis of nitrogen adsorption-desorption measurements was performed to determine the specific surface area, porosity, and surface roughness factor for the HRTA materials, with the isotherm shown in Fig. S1(d) and the data summarized in Table S1. The average specific surface area, porosity, and roughness factor of HRTA were calculated to be 84 m^2g^{-1}, 62.0 % and 137.3 μm^{-1}, respectively. This is important given the previously mentioned concerns regarding dye loading.

Films of nanocrystalline HRTA particles were manually doctor-bladed onto F-doped SnO_2 (FTO) glass substrates, with different pressures to yield different film thicknesses. These were used as the mesoporous working electrodes. Films were sintered and sensitised with either

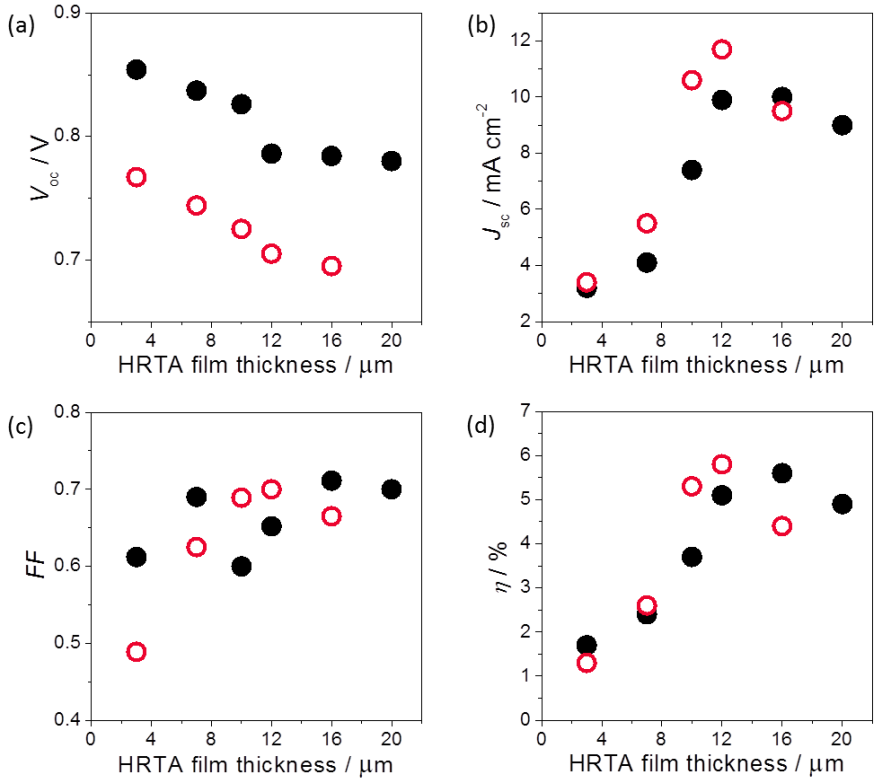

Figure 2. Photovoltaic characteristic of DSCs containing N719-based (black solid dots) and D149-based (red open dots) sensitizers as a function of nanocrytalline HRTA film thickness: (a) open-circuit voltage, V_{oc}, (b) short circuit photocurrent density, J_{sc}, (c) fill factor, *FF*, and (d) solar-to-electric energy conversion efficiency, η.

D149 or N719 before being assembled into devices with a Pt-loaded counter electrode and iodide-triiodide (I^-/I_3^-) based electrolyte.

Current density-voltage results obtained under one sun illumination [air mass 1.5 global (AM 1.5G), 100 mW cm^{-2}] are shown in Figure 2, with key photovoltaic parameters summarized in Table S2. The open-circuit voltage [V_{oc}, Figure 2(a)] decreases for both the N719- and the D149-based DSCs with increasing HRTA film thickness, as per expectation, since (1) charge density, and hence the quasi Fermi level, decreases because the injected electrons are distributed throughout a larger volume and there are diminishing returns with regards to light harvesting; and (2) the increased material surface area leads to more opportunities for charge-recombination to occur.

In contrast, the short circuit phototocurrent densities (J_{sc}) [Figure 2(b)] increase up to a maximum value, before decreasing again for thicker HRTA films. For N719-based DSCs, J_{sc} increases continuously with film thickness from 3 µm to 16 µm, reaching a maximum value of 10.0 mA cm^{-2} (leading to a maximum η of 5.6 %, up from 5.3%), while D149-based DSCs attain their highest J_{sc} at 12 µm (just under 12 mA cm^{-2}, giving an overall conversion efficiency of 5.8 %). Aside from the thinnest D149-sensitized device, all revealed *FF* values in the range of 0.65 ± 0.5, with no strong dependence observed.

Incident photon-to-current conversion efficiency (IPCE) spectra of DSCs with N719 and D149 dyes are presented in the inset of Figure 3(a). Higher IPCE values were obtained for D149-based DSCs than for N719-based DSCs; the peak IPCE values were observed at 535 nm for N719 and D149, reaching 54 % and 68 %, respectively. The D149-based DSCs have an impressive response over a wide spectral range; the IPCE values exceeded 60 % from 450 to 650 nm, resulting in the high J_{sc} value observed (~ 12 mA cm^{-2}). The average IPCE of the N719-based DSCs was 14 % lower than that of the D149-based DSCs from 350 to 650 nm, in

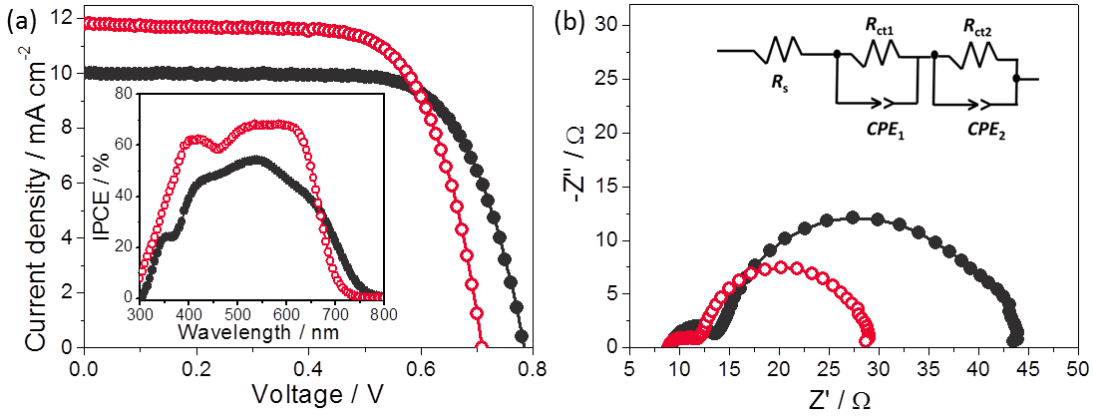

Figure 3. (a) *I-V* curves, inset: IPCE spectra, (c) Nyquist plots, inset: the equivalent circuit for DSCs with N719-based (black solid dots) and D149-based (red open dots) sensitizers (light intensity: 100mA cm^{-2}, AM 1.5).

contrast to the much wider photo-response range and much higher IPCE values for D149-based DSCs.

To better understand the electron transport properties in N719 and D149 sensitized DSCs, electrochemical impedance spectroscopy (EIS) measurements were performed at V_{oc} under 1 sun illumination (with both devices having a HRTA thickness of 10 µm), as shown in Figure 3(b), with the equivalent circuit in the inset. The large semicircle in the Nyquist plots at low frequency corresponds to the charge transfer resistance at the photoanode TiO_2/dye/electrolyte interface. It can be seen that the resistance at the TiO_2/D149/electrolyte interface is much smaller than that of the TiO_2/N719/electrolyte interface. Thus, the efficient charge transfer at the TiO_2/D149/electrolyte interface, combined with the higher extinction coefficient of D149 may synchronously contribute to higher J_{sc} and η for the D149-based DSCs.

Conclusion

3D hierarchical rutile architecture (HRTA) particles were successfully synthesized by a modified facile hydrothermal method, optimized for use in DSC photoanodes. N719 and D149 (a metal-free indoline dye) were compared as sensitizers, with efficiencies of 5.6 % and 5.8 % achieved for 16 µm-thick and 12 µm-thick films, for N719- and D149-based DSCs, respectively. The improved performance could be explained by enhanced light harvesting and

reduced electron transfer resistance. Not only does this show that rutile TiO_2 may be a viable material for use in DSCs, but it also shows the importance of viewing the DSC as a system rather than simply focusing on the individual components therein.

Supporting Information (SI)

A Comparative Study of N719- and D149-sensitized 3D Hierarchical Rutile TiO_2 Solar Cells

Jianjian Lin,[a] Yoon-Uk Heo,[b] Andrew Nattestad,[c,*] Yusuke Yamauchi,[d] Shi Xue Dou,[a] and Jung Ho Kim[a,*]

[a]*Institute for Superconducting and Electronic Materials (ISEM), Australian Institute for Innovative Materials (AIIM), University of Wollongong, North Wollongong, NSW 2500, Australia*
Tel: +61-2-4298-1420. E-mail: jhk@uow.edu.au
[b]*Graduate Institute of Ferrous Technology, Pohang University of Science and Technology, San 31, Hyoja-Dong, Pohang 790-784, Republic of Korea*
[c]*Intelligent Polymer Research Institute (IPRI), ARC Centre of Excellence for Electromaterials Science, AIIM, University of Wollongong, North Wollongong, NSW 2500, Australia*
Tel: +61-2-4298-1456. E-mail: anattest@uow.edu.au
[d]*World Premier International (WPI) Research Center for Materials Nanoarchitectonics (MANA), National Institute for Materials Science (NIMS), 1-1 Namiki, Tsukuba , Ibaraki 305-0044, Japan*

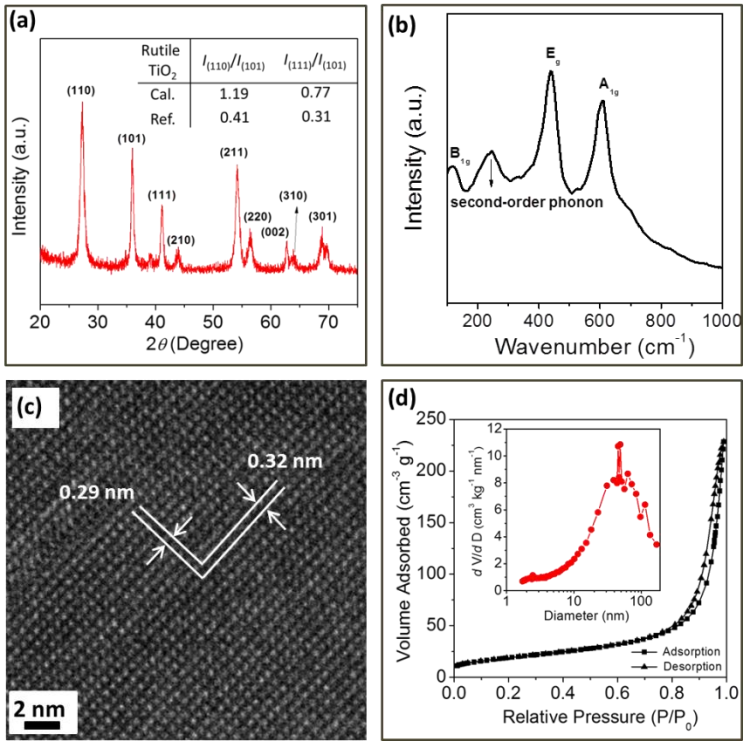

Figure S1. (a) XRD pattern of HRTA, which can be indexed to a pure rutile TiO_2 crystal structure (JCPDS No. 21-1276; space group $P4_2/mnm$; a = 0.45927 nm, c = 0.29544 nm), with diffraction intensity ratios of HRTA and the reference sample[ref] in the inset table. ($I_{(110)}/I_{(101)}$ and $I_{(111)}/I_{(101)}$ stand for the intensity ratios of the (110) to (101) and (111) to (101) peaks, respectively. (b) Raman spectrum of as-prepared HRTA, indicating that the as-prepared sample possesses rutile phase according to the characteristic Raman modes at 118 cm^{-1} (B_{1g}), 438 cm^{-1} (E_g), and 607 cm^{-1} (A_{1g}) with a broad band near 240 cm^{-1} assigned to a second-order photon. (c) HRTEM image showing the fringe spacings of rutile TiO_2 nanocrystal, with two kinds of fringes perpendicular to each other with d-spacings of 0.29 nm and 0.32 nm, which can be readily ascribed to the lattice spacings of the (001) and (110) planes, and is consistent with the d values of the (001) and (110) planes of the tetragonal rutile TiO_2, respectively. (d) N_2 adsorption-desorption isotherms of the HRTA; inset: corresponding pore size distribution calculated by the Barrett-Joyner-Halenda (BJH) method from the adsorption branch.

Table S1 Specific surface area, porosity, and roughness factor of 3D hierarchical rutile TiO_2 architecture (HRTA) material compared to a previous report (HRT-1).[ref]

Samples	Specific surface area ($m^2\ g^{-1}$)	Porosity [a)] (%)	Roughness factor [b)] (μm^{-1})
HRTA	84	62.0	137.3
HRT-1	67	56.6	125

[a)] The porosity (P) of HRTA was calculated according to: $P = V_p / (q^{-1} + V_p)$, where V_p is the specific cumulative pore volume ($cm^3\ g^{-1}$) and q is the density of TiO_2 (q = 4.3 $g \cdot cm^{-3}$).

[b)] An estimation of the roughness factor (R) per unit film thickness of the films is obtained by $R = q\ (1\text{-}P)\ S$, where q is the density ($g\ cm^{-3}$) of TiO_2, P is the porosity (%) of the film, and S is the specific surface area ($m^2\ g^{-1}$).

Table S2 Photovoltaic parameters of N719- and D149-based DSCs measured under air mass (AM) 1.5 global (1.5G) one sun illumination (100 mW cm^{-2}). J_{sc}: short-circuit photocurrent density; V_{oc}: open-circuit photovoltage; *FF*: fill factor; η: total power conversion efficiency. The active areas were ~ 0.16 cm^2 for all of the cells (with the mask area 0.25 cm^2).

Samples	Film thickness[a)] (μm)	J_{sc} (mA cm^{-2})	V_{oc} (V)	*FF* (%)	η (%)
N719-DSCs	3	3.2	0.854	61.2	1.7
	7	4.1	0.837	69.0	2.4
	10	7.4	0.826	60.0	3.7
	12	9.9	0.786	65.2	5.1
	16	10.0	0.784	71.1	5.6
	20	9.0	0.780	70.0	4.9
D149-DSCs	3	3.4	0.767	48.9	1.3
	7	5.5	0.744	62.5	2.6
	10	10.6	0.725	68.9	5.3
	12	11.7	0.705	70.0	5.8
	16	9.5	0.695	66.5	4.4

[a)] Measurement of film thickness was carried out on a surface profile system (Veeco Dektak 150).